

FLAMMABILITY AND BURNING RATES OF LOW QUALITY BIOGAS AT ATMOSPHERIC CONDITION

Mohd Suardi Suhaimi^a, Aminuddin Saat^{b*}, Mazlan Abdul Wahid^b

^aDepartment of Chemical Engineering, Faculty of Chemical Engineering, Universiti Teknologi Malaysia, 81310 UTM Johor Bahru, Johor, Malaysia

^bDepartment of Thermofluids, Faculty of Mechanical Engineering, Universiti Teknologi Malaysia, 81310 81310 UTM Johor Bahru, Johor, Malaysia

Article history

Received

21 January 2017

Received in revised form

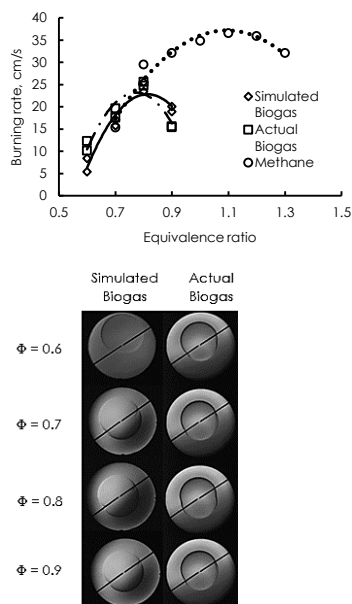
31 May 2017

Accepted

17 August 2017

*Corresponding author
amins@mail.fkm.utm.my

Graphical abstract



Abstract

This study focuses on the flammability and burning rate of simulated and actual biogas-air mixture for equivalence ratio of 0.5 to 1.0. The content of simulated biogas was set at 50% CH₄ and 50% CO₂ to emulate the typical composition of low quality biogas. Studies on low quality biogas combustion with this particular CH₄ and CO₂ content are still scarce in literature. It was found that the flammability limits fall within the same range for both simulated and actual biogas from 0.6 to 0.9 which is substantially narrower compared to pure methane. Incidence of flame buoyancy were observed for both simulated and actual biogas at equivalence ratio of 0.6 and 0.7. The maximum burning rates were almost identical for simulated and actual biogas at 21.18 cm/s and 24.74 cm/s respectively. It was also found that the peak of burning rate occurs at the leaner equivalence ratio of 0.8 for both simulated and actual biogas. These observations imply the significance of CO₂ on biogas combustion. Compared to pure methane, the reduction in burning rate and the shift in the peak burning rate to the leaner mixture suggest the physical and chemical effects of CO₂ on biogas combustion. Physically, the presence of CO₂ could adversely affect the temperature driven CH₄ preferential diffusion into the reaction zone since CO₂ could absorb some of the heat released during combustion. When present at 50% or higher, CO₂ could significantly reduce OH radical formation thereby narrowing the flammability limits and reducing the burning rates.

Keywords: Actual biogas, simulated biogas, flammability limit, buoyancy, burning rate

© 2017 Penerbit UTM Press. All rights reserved

1.0 INTRODUCTION

Biogas mainly composed of around 50-70% methane and 30-50% carbon dioxide with trace gases at smaller quantity. Naturally, it is produced by anaerobic fermentation of various wastes ranging from municipal to agricultural. Due to its renewability, biogas could be the energy of the future as an alternative to the depleting fossil fuel. Exploiting biogas can also help to

reduce Green House Gasses emission as its combustion generates smaller pollutants than fossil fuels [1]. Due to its promising future, numerous studies are directed towards biogas production and processing. These includes the optimization of methanogenesis, purification and enrichment. However, studies on biogas combustion characteristics are relatively scarce. Knowledge combustion characteristics is vital to optimize the use

of biogas [2]. It is also useful to provide data for numerical studies and also in the design of practical combustors. One notable problem in biogas combustion is the interaction between CH_4 and CO_2 that could cause irregular combustion characteristics that may complicate the commercial use of biogas [3].

Flammability limits, flame speed, Markstein length and laminar burning rate are among the fundamental combustion characteristics that are used to describe both the laminar and turbulent premixed combustion of certain fuels. Accurate measurement of laminar premixed flames permits the understanding of propagation rates, heat release, quenching and emission characteristics. Knowledge from laminar premixed flame is also essential in understanding turbulent nonpremixed combustion, which is a much more complex combustion phenomenon normally found in practical combustors. Usually, the initial stage of this type of combustion is dominated by laminar premixed combustion.

The aforesaid combustion characteristics could be derived from data of flame speed. There are several methods to determine flame speed such as flat flame [4, 5], counterflow flame [6, 7] and spherically expanding flame [8-11]. The latter constitutes the most versatile and accurate method to date [12]. The laminar flame speed of spherically expanding flame can be obtained from schlieren photographs as described by Bradley *et al.* [13]. The determination of laminar flame speed enables the determination of unstretched laminar flame speed, stretch and burning rate [13]. Laminar burning rate is defined as the normal velocity of the cold reactants movement into the reaction zone [13].

Flammability limits refers to the equivalence ratio limits at which flame could be initiated and propagate. Different fuel could have different flammability limits due to difference in fuel chemistry [14]. Wider limits is favorable as it implies that such fuel is flammable over a wider range of equivalence ratio. It could also be altered by different initial conditions such as pressure and temperature even for the same fuel. Buoyancy is the phenomenon where flame displays density stratification in the opposite direction of body force such as gravity. It could also lead to instability known as Rayleigh-Taylor instability.

Most studies in literature focused on biogas with methane content of more than 60% often termed as high quality biogas [15]. Relatively lesser attention are given on biogas with 50% or lower methane content (often termed as low quality biogas). Studying low quality biogas combustion characteristics could justify if unrefined low quality biogas could be directly used in commercial combustors as the cost of enriching biogas is quite high [16]. The objective of this study is to determine the flammability limits, burning rate and the flame behavior of actual and simulated biogas-air mixture using images from Schlieren photography. The contents of actual and simulated biogas is shown in Table 1. Schlieren photography enables the detection of density gradient resulting from combustion. It also

permits the exclusion cellular flames that render the smooth flame front assumption void.

2.0 METHODOLOGY

The experimental setup comprising a 29.3L cylindrical constant volume combustion chamber (CVCC) with two 190mm optical windows arranged at the centre of a linear Schlieren photography setup is shown in Figure 1. The cylindrical CVCC is equipped with a pair of opposing spark electrodes connected to ignition box providing ignition at the centre. The linear Schlieren setup arrangement consisted of 150 mm collimating and focusing lens, an LED light source and Phantom 7.1 high-speed camera. After the CVCC was vacuumed, it was filled either with actual biogas or methane and CO_2 mixture in case of simulated biogas and air with different partial pressure that correspond to the desired equivalence ratio ranging from 0.5 to 1.0. The content of actual biogas was characterized using gas chromatography and tabulated in Table 1. Trace gasses are usually composed of N_2 and H_2S [11]. The initial pressure for each experiment was set at atmospheric pressure with initial temperature range of 298-302K. Ignition was controlled via a desktop computer (with LabView 7.1 software) connected to the ignition box. The images of spherically expanding flames were recorded by Phantom 7.1 high-speed camera connected to a notebook PC after mixtures of either simulated or actual biogas were ignited. The images were then analyzed using image processing softwares (Adobe Photoshop CS4 and Matlab 2014) to determine the equivalent flame radius. Flame speed of each fuel was obtained by differentiation of flame radius with respect to time.

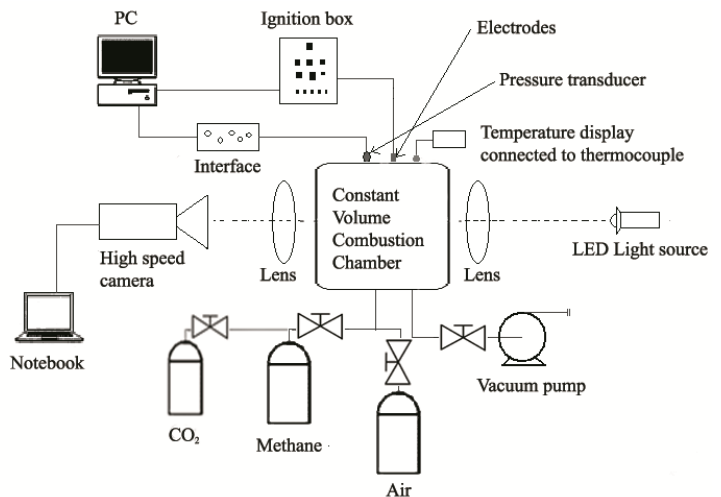


Figure 1 Experimental setup

Table 1 Composition of simulated and actual biogas for current study

Gas	Simulated Biogas		Actual Biogas		
	CH ₄	CO ₂	CH ₄	CO ₂	Other
Percentage (%)	50	50	49-52	48-51	0.3-1.1

3.0 RESULTS AND DISCUSSION

The images of spherical flame at a radius of approximately 40 mm for different equivalence ratio of both fuels are shown in Figure 2. Notably at equivalence ratio of 0.6, the flame of simulated biogas exhibits a much more prominent buoyancy compared to the actual biogas. As there is only a slight difference in methane and CO₂ between both fuels, this observation suggest that a slight difference in content could give rise to a significant difference in combustion for mixture closer to lean limit. The mixture of 0.7 also experienced buoyancy but not as obvious as 0.6. No buoyancy could be observed for the mixture of 0.8 and 0.9. Generally, weak flames are more susceptible to buoyancy that could also affect flame morphology complicating image processing and analysis [17]. It could lead to a form of instability commonly termed as the Rayleigh-Taylor instability. For a spherically expanding flame, the portion of the flame that propagates downward could be subjected to this kind of instability. Moreover, if the thickness of the flame is sufficiently low, cellularity could occur [17]. In this study however, no cellularity was observed for all of the mixtures indicating that the thickness is sufficiently high to inhibit cellularity. A slightly ellipsoidal shape of actual biogas flame could be due to the position of the electrodes that could change slightly due to air movement during combustion.

Figure 3 shows the difference in flame propagation speed for actual and simulated biogas for the equivalence ratio of 0.6. During the first ten millisecond after ignition, the flame speed of both flame exhibit typical reduction caused by diminishing radicals from spark that ignites the mixtures. This region often described as the spark affected region. The flame then started to stabilize to reach a steady flame speed towards the end of combustion. Thus, in terms of trend, the flame speed of both fuels are almost identical. However, in terms of magnitude, the difference in flame speed between both fuels are quite significant at around 32%. Such noticeable difference could be attributed to a slight difference in actual biogas methane content which is slightly higher at 52% and lower CO₂ at 47% together with approximately 1% of trace gasses. The kinetics is apparently sensitive to fuel content at this particular equivalence ratio [3].

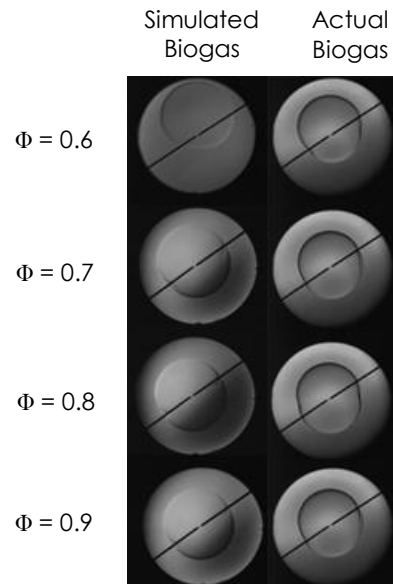
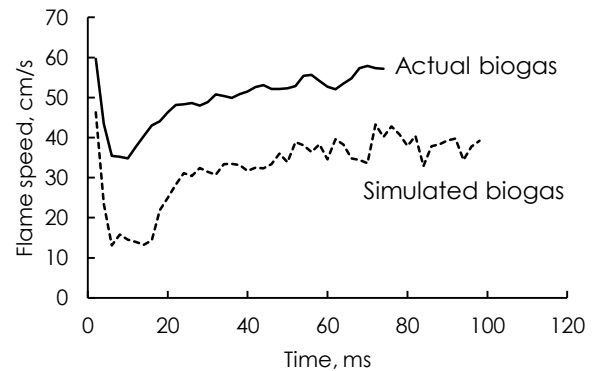
**Figure 2** Flame images at radius of approximately 40mm for both fuels across the equivalence ratio**Figure 3** Comparison of actual and simulated biogas flame speed duplicate experiments for the mixture of $\phi = 0.6$

Figure 4 shows the variation of flame speed with time for the biogas mixture at equivalence ratio of 0.8. During the spark affected region, there is a significant difference of flame speed between simulated and actual biogas flame. However, as the combustion progress towards a steady flame speed, the difference started to diminish to the extent that it has become negligible. At this particular equivalence ratio, such small differences in biogas and simulated biogas content started to become insignificant compared to the flame of equivalence ratio 0.6. As the volume of methane and CO₂ increases, the kinetics of combustion would depends on different rate determining step [3]. This would be explained further in the discussion of burning rate.

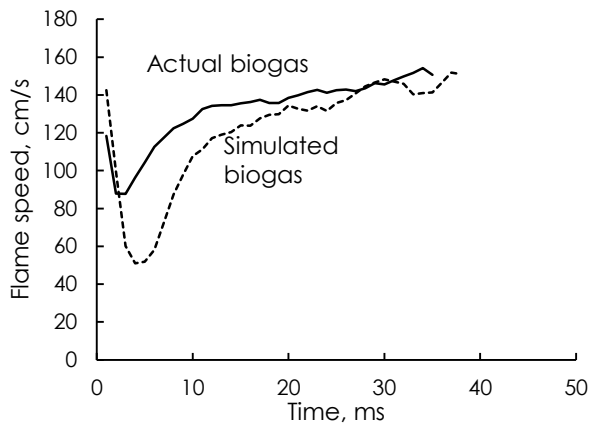


Figure 4 Variation of flame speed with time for biogas mixture at equivalence ratio of 0.8

Markstein length indicates the extent at which the flame speed is affected by stretch. Larger magnitude of Markstein length indicates a flame that is more amenable to the effect of stretch and better stability. In the case of spherically expanding flame, stretch is contributed by both flame curvature and aerodynamic strain. Figure 5 shows the difference in the magnitude of Markstein length between simulated, actual biogas and pure methane [18]. The overall trend of Markstein length variation with equivalence ratio is almost identical for pure methane, simulated and actual biogas where it increases with equivalence ratio. This could be attributed to the density ratio of the unburned to the burned gas that increases proportionately to equivalence ratio followed by a decrease in flame thickness [19]. The difference being the degree at which the increment in Markstein length occur. Markedly, the increase is much more apparent for both actual and simulated biogas compared to pure methane suggesting a more significant role of stretch as equivalence ratio increases. At equivalence ratio of 0.7, the Markstein length for simulated and actual biogas are noticeably higher than that of pure methane. This trend continues as equivalence increase to 0.9 where the Markstein length of both simulated and actual biogas deviate further from that of pure methane. Apparently the presence of CO_2 could significantly enhance the effect of stretch on flame propagation.

Increase in Markstein length also indicates a change in mass-thermal diffusion. Diffusion is a transport process that is driven by difference in concentration (fickian), molecular weight (preferential) or temperature (soret). Due to the presence of CO_2 that has different molecular weight and heat capacity, modification on the aforesaid types of diffusion could be expected. Compared to methane CO_2 has higher molecular weight and heat capacity, thus when present especially at sufficiently high amount, could alter the concentration and

temperature gradient, as well as diffusion of methane and O_2 into the reaction zone [20].

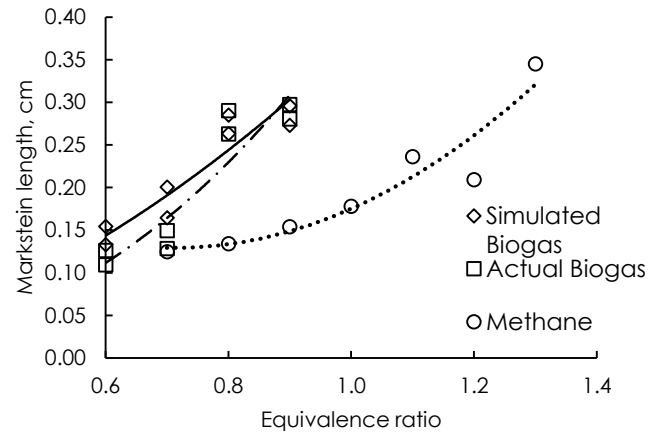


Figure 5 Variation of Markstein length at wide range of equivalence ratio for biogas and methane

Thermal diffusion from the reaction zone (flame), could be enhanced by CO_2 due to its higher heat capacity. This often termed as dilution effect [11]. Such increase in thermal diffusion could consequently increase the Lewis number and Markstein length and decrease the flame adiabatic temperature. This effect could also modify methane diffusion into the reaction zone. Positively stretched flame such as in the outwardly propagating flame could also reduce the effect of preferential diffusion [20]. This could further hamper the transport of methane and oxygen into the reaction zone, contributing to an increase in Lewis number.

Figure 6 shows the variation of burning rate of pure methane, actual biogas and simulated biogas-air mixture over a wide range of equivalence ratios. Burning rate is the product of unstretched flame speed (obtained through extrapolation of flame speed to the point of zero stretch) and the burned and unburned gas density ratio. Data of the early stage of combustion could be omitted as these data are mostly influenced by ignition energy and could result in over or underestimation of unstretched flame speed. With the exception of the magnitude and shift in the peak, the burning rates for all the fuel share the quadratic variation with equivalence ratio. There are obvious differences in burning rate magnitude and the corresponding equivalence ratio at which the peak of the burning rate occur between both actual and simulated biogas and pure methane. The maximum burning rate of both simulated and actual biogas occurs at equivalence ratio of 0.8 at around 22-25 cm/s, a significant variation from pure methane at approximately 37 cm/s at equivalence ratio of 1.1. Previous studies reported a slightly higher burning rate of 27 cm/s at equivalence ratio of 1.0 for actual biogas [21 & 22].

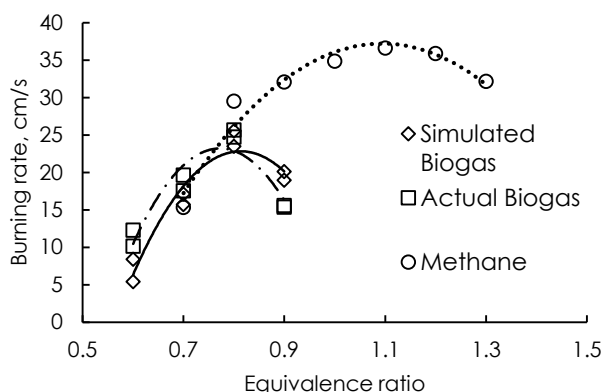


Figure 6 Variation of burning rate at wide range of equivalence ratio for biogas and methane

The reduction of burning rate is a direct effect of CO_2 . Pure methane contains no CO_2 while the actual and simulated biogas contains 48-51% and 50% of CO_2 respectively. CO_2 could thermally and chemically affect simulated biogas combustion. Thermally, CO_2 could absorb some of the heat released during combustion thus reduce burning rate due to its higher heat capacity [11]. While, chemically it could reduce the rate at which OH radicals produced [3; 23; 24]. In terms of chemical effect, when CO_2 are present at 50% or more, significant change in kinetics would occur especially for leaner mixture [3]. This would involve the reduction of certain radicals that vital in sustaining combustion. OH radicals are important during the chain branching reaction during combustion. As the equivalence ratio increases (and also CO_2), direct decomposition of methane contained in the actual and simulated biogas plays a much more important role in ignition and combustion. This could explain why both actual and simulated biogas could not be ignited at equivalence ratio higher than 0.9. Direct decomposition of methane produces CH_3 and H radicals in contrast to OH and CH_3O radicals. Intuitively, as CH_3 increases, the likelihood of this radicals to recombine also increases, and further contribute to the inhibition of combustion.

4.0 CONCLUSION

In the present work, the combustion of actual and simulated biogas have been studied by analyzing their spherically propagating flame. From the flame images, highest flame speed hence the burning rate was observed at equivalence ratio of 0.8 for both simulated and actual biogas. Compared to pure methane, the calculated burning rate shows a significant reduction and shift from the maximum point at equivalence ratio of 0.8. The reduction in burning rate could be linked to the presence of CO_2 . The shift in the peak of burning rate to leaner equivalence ratio

has also been reported previously in literature albeit under this particular condition the shift is more apparent. The flammability limits are also much narrower compared to data from literature. Consideration of flammability limits is important in the design of practical combustors to avoid the problem of misfiring that could reduce performance and increase fuel consumption. An increase in flame sensitivity to stretch, which also known as Markstein length was also observed when CO_2 are present, indicating alteration in mass and heat transport by CO_2 and flame sensitivity to the effect of stretch. These observations could serve as primary data for numerical or experimental studies on much more complex flame configurations particularly those involving turbulence that normally occurs in practical combustors. Therefore, this would also help in the design of practical combustors that are suited to biogas.

Acknowledgement

The authors would like to thank Ministry of Science, Technology and Innovation of Malaysia (MOSTI) and Universiti Teknologi Malaysia for supporting this research activity under the Research Grant Scheme No. R.J130000.7824.4F749.

References

- [1] Schoen, E. J. and D. M. Bagley. 2012. Biogas Production and Feasibility of Energy Recovery Systems for Anaerobic Treatment of Wool-Scouring Effluent. *Resources, Conservation and Recycling*. 62: 21-30.
- [2] Meighalchi, M., J. C. Keck. 1980. *Combustion and Flame*. 38: 143-154.
- [3] Fischer, M., Jiang X. 2015. An Investigation of the Chemical Kinetics of Biogas Combustion. *Fuel*. 150: 711-720.
- [4] Bosschaart, K. J., de Goey, L. P. H. 2004. The Laminar Burning Velocity of Flames Propagating in Mixtures of Hydrocarbons and Air Measured with the Heat Flux Method. *Combustion and Flame*. 136: 261-269.
- [5] Konnov, A. A., Dyakov, I. V., De Ruyck, J. 2003. Measurement of Adiabatic Burning Velocity in Ethane-Oxygen-Nitrogen and in Ethane-Oxygen-Argon Mixtures. *Exp. Therm. Fluid Sci*. 27: 379-384.
- [6] Chao, B. H., Egolfopoulos, F. N., Law, C. K. 1997. Structure and Propagation of Premixed Flame in Nozzle-generated Counterflow. *Combustion and Flame*. 109: 620-638.
- [7] Jackson, G. S., Sai, R., Plaia, J. M., Boggs, C. M., Kiger, K. T. 2003. Influence of H_2 on the Response of Lean Premixed CH_4 Flames to High Strained Flows. *Combustion and Flame*. 132: 503-511.
- [8] Taylor, S. C. 1991. Burning Velocity and the Effect of Flame Stretch. PhD Thesis. University of Leeds.
- [9] Hassan, M. I., Aung, K. T., Faeth, G. M. 1998. Measured and Predicted Properties of Laminar Premixed Methane/Air Flames at Various Pressures. *Combustion and Flame*. 115: 539-550.
- [10] Gu, X. J., Haq, M. Z., Lawes, M., Woolley, R. 2000. Laminar Burning Velocity and Markstein Lengths of Methane-air Mixtures. *Combustion and Flame*. 121: 41-58.
- [11] Hinton, N., Stone, R. 2014. Laminar Burning Velocity Measurements of Methane and Carbon Dioxide Mixtures

- (Biogas) Over Wide Ranging Temperatures and Pressures. *Fuel*. 116: 743-750.
- [12] Bradley, D., Hicks, R. A., Lawes, M., Sheppard, C. G. W., and Woolley, R. 1998. The Measurement of Laminar Burning Velocities and Markstein Numbers for Iso-octane-Air and Iso-octane-nHeptane-Air Mixtures at Elevated Temperatures and Pressures in an Explosion Bomb. *Combustion and Flame*. 115(1-2):126-144.
- [13] Gillespie, L., Lawes, M., Sheppard, C. G. W., and Woolley, R. 2000. Aspects of Laminar and Turbulent Burning Velocity Relevant to SI Engines. Society of Automotive Engineers.
- [14] Pizutti, L., Martins, C. A., Lacava, P. T. 2016. Laminar Burning Velocity and Flammability Limits in Biogas: A Literature Review. *Renewable and Sustainable Energy Reviews*. 62: 856-865.
- [15] Zhen, H. S., Leung C. W., Cheung C. S. 2013. Effects of Hydrogen Addition on the Characteristics of a Biogas Diffusion Flame. *International Journal of Hydrogen Energy*. 38: 6874-81.
- [16] Moghaddam, E. A., Ahlgren S., Hultberg, C., Nordberg, Å. 2015. Energy Balance and Global Warming Potential of Biogas-based Fuels from a Life Cycle Perspective. *Fuel Processing Technology*. 132: 74-82.
- [17] Law, C. K. 2006. *Combustion Physics*. Cambridge University Press.
- [18] Suhaimi, M. S., Saat, A., Wahid, M. A., Sies, M. M. 2016. Flame Propagation and Burning Rates of Methane-Air Mixtures Using Schlieren Photography. *Jurnal Teknologi*. 78(10-2)21-27.
- [19] Miao, H., Liu, Y. 2014. Measuring the Laminar Burning Velocity and Markstein Length of Premixed Methane/Nitrogen/Air Mixtures with the Consideration of Nonlinear Stretch Effects. *Fuel*. 121: 208-215.
- [20] Liang, W., Chen, Z., Yan, F., Zhang, H. 2013. Effects of Soret diffusion on the Laminar Flame Speed and Markstein length of Syngas/Air Mixtures. *Proceedings of the Combustion Institute*. 34: 695-702.
- [21] Cardona C, Amell AA. 2013. Laminar Burning Velocity and Interchangeability Analysis of Biogas/C₃H₈/H₂ with Normal and Oxygen-enriched Air. *International Journal of Hydrogen Energy*. 39: 7994-8001.
- [22] Anggono, W., Wardana, I. N. G., Lawes, M., Hughes, K. J. 2014. Effect of Inhibitors on Biogas Laminar Burning Velocity and Flammability Limits in Spark Ignited Premix Combustion. *International Journal of Engineering and Technology (IJET)*. 5(6): 4980-4987.
- [23] Qiao, L., Gan, Y., Nishiie, T., Dahm, W. J. A., Oran, E. S. 2010. Extinction of Premixed Methane/Air Flames in Microgravity by Diluents: Effects of Radiation And Lewis Number. *Combustion and Flame*. 157: 1446-1455.
- [24] Mameri, A., Tabet, F. 2016. Numerical Investigation of Counter-flow Diffusion Flame of Biogas-hydrogen Blends: Effects of Biogas Composition, Hydrogen Enrichment and Scalar Dissipation Rate on Flame Structure and Emissions. *International Journal of Hydrogen Energy*. 41: 2011-2022.